

---

Faculty of Science

Faculty Publications

---

Disassembly of an epibenthic assemblage in a sustained severely hypoxic event in a northeast Pacific basin

Ryan Gasbarro, Jackson W.F. Chub, Verena Tunnicliffe

October 2019

© 2019 The Authors. Published by Elsevier B.V. This is an open access article under the CC BY-NC-ND license ( <http://creativecommons.org/licenses/by-nc-nd/4.0/> ).

This article was originally published at:

<https://doi.org/10.1016/j.jmarsys.2019.103184>

---

Citation for this paper:

Gasbarro, R., Chu, J.W.F. & Tunnicliffe, V. (2019). Disassembly of an epibenthic assemblage in a sustained severely hypoxic event in a northeast Pacific basin.

*Journal of Marine Systems*, 198, 103184.

<https://doi.org/10.1016/j.jmarsys.2019.103184>



## Disassembly of an epibenthic assemblage in a sustained severely hypoxic event in a northeast Pacific basin



Ryan Gasbarro<sup>a,c,\*</sup>, Jackson W.F. Chu<sup>b,d</sup>, Verena Tunnicliffe<sup>a,b</sup>

<sup>a</sup> School of Earth & Ocean Sciences, University of Victoria, PO Box 1700, Victoria, BC V8W 2Y2, Canada

<sup>b</sup> Department of Biology, University of Victoria, PO Box 1700, Victoria, BC V8W 2Y2, Canada

<sup>c</sup> Department of Biology, Temple University, 1900 N. 12<sup>th</sup> Street, Philadelphia, PA, USA

<sup>d</sup> Department of Ocean Sciences, Memorial University of Newfoundland, 0 Marine Lab Road, St. John's, NL A1C 5S7, Canada

### ARTICLE INFO

#### Keywords:

Oxygen  
Species associations  
Ecological time-series  
Saanich Inlet  
Hypoxia

### ABSTRACT

As global ocean deoxygenation proceeds and the frequency of extreme low-oxygen (hypoxic) events increases, seafloor ecosystems will inevitably be affected. Our study examines how benthic community responses scale with the severity and spatial extent of hypoxia. Saanich Inlet is a natural model system for testing the effects of hypoxic conditions that determine the benthic megafaunal community structure during annual deoxygenation and reoxygenation. In 2016, an anomalously severe and widespread hypoxic event occurred in the fjord after a decade of oxygen decline at a rate of  $0.07 \text{ mL L}^{-1} \text{ y}^{-1}$  as measured by a cabled seafloor observatory. We use a living ecological time-series generated from remotely operated vehicle surveys to assess how the benthic megafaunal community disassembled in response to this extreme hypoxic event. Three benthic surveys at similar times in 2013 and 2016 reveal large increases in the area of seafloor bathed in anoxic and hypoxic waters in the latter year. Both bottom oxygen and species depth distributions shoaled from 2013 to 2016, accompanied by a 56% overall decline in megafauna. The abundant habitat-forming pennatulacean octocoral, *Halipteris willemoesi*, decreased in abundance by 92.3% from fall 2013 to fall 2016, and pandalid shrimp disappeared from the community. Hypoxia-tolerant species experienced milder losses, and two new species occurred in 2016 – one a predator on the coral. Co-occurrence analyses revealed loss of significant community segregation from 2013 to 2016, and a re-mix of pairwise species co-occurrences in the latter year. The loss of oxygenated habitat compressed species into narrower depth ranges and led to disassembly probably through niche space constriction, while decimation of some populations eliminated key community associations. Community fragmentation and disruption of interactions is a possible outcome for many marine benthic ecosystems as marine hypoxia intensifies.

### 1. Introduction

Climate change is manifest in the ocean through deoxygenation, shifting thermal regimes, and acidification, all of which may act as cumulative stressors on marine ecosystems (Doney et al., 2012). The consequences for changes in biodiversity and ecosystem functioning could be profound (Cardinale et al., 2012), but accurate predictions of such shifts remain elusive. Species richness contributes to community resistance to pathogens and invasion, as well as its ability to recover from disturbance (Giller and O'Donovan, 2002; Worm et al., 2006). However, not all species contribute equally to these functions. The loss of highly connected and/or abundant 'generalist' species in the complex networks of ecosystems creates cascading effects and fragmentation (Albert and Jeong, 2000; May et al., 2008; Bascompte and Stouffer,

2009). Conversely, rare species can occupy singular functional spaces (Leitao et al., 2016; Chapman et al., 2018); thus these losses may have large consequences. We can, therefore, improve predictions about ecological consequences of ocean change through study of how climate-related stressors exclude species from communities, and how the surviving taxa respond.

Community disassembly is the nonrandom, stepwise process of abundance decline, species extirpation (i.e. local extinction), range contraction, and change in interaction network; in contrast, assembly is the temporal integration of species into a community (Zavaleta et al., 2009). Evidence from mathematical models (Post and Pimm, 1983; Drake, 1990), microcosm manipulations (Drake, 1991), and freshwater ponds (Chase, 2003; O'Neill, 2016) describes multiple endpoints of community structure dependent on assembly history. However, the

\* Corresponding author.

E-mail address: [ryan.gasbarro@temple.edu](mailto:ryan.gasbarro@temple.edu) (R. Gasbarro).

<https://doi.org/10.1016/j.jmarsys.2019.103184>

Received 23 January 2019; Received in revised form 15 May 2019; Accepted 27 May 2019

Available online 01 June 2019

0924-7963/ © 2019 The Authors. Published by Elsevier B.V. This is an open access article under the CC BY license (<http://creativecommons.org/licenses/by/4.0/>).

pattern of community disassembly is not simply assembly in reverse, and the order of declines/losses is a significant factor in determining the endpoint(s) of the process (Saavedra et al., 2008; O'Neill, 2016). While theory posits that ecosystems may be resilient when rare species disappear, and sensitive to the loss of abundant species due to their highly interconnected nature (Olesen et al., 2008; Bascompte and Stouffer, 2009), a growing body of evidence describes critical functional contributions from rare species (Leitao et al., 2016) that may be among the first eliminated during the disassembly process (Purvis, 2000). Fewer species co-occur as species abundances approach zero, leading to disruptions in the competitive and trophic structure of the community (Belyea and Lancaster, 1999; Zavaleta et al., 2009). Some species benefit from increased resource availability (Johnson et al., 1996) while others experience increased competition in a compressed (i.e. fewer linkages between species) co-occurrence space (Zavaleta et al., 2009).

In the majority of disassembly studies, causal agents are anthropogenic, either directly or against a background of human pressures (Springer et al., 2003; Darling et al., 2013; Daskalov et al., 2017). Here, model-based and manipulative studies provide insights into the outcomes of community disassembly; however, because observational time-series documenting this phenomenon are rare, it is unclear whether predictions from such studies translate into natural settings. Ocean deoxygenation is a climate-related stressor (Keeling et al., 2010; Levin, 2018) that drives responses at multiple levels of biological organization ranging from the physiological and biochemical (Pörtner, 2010; Seibel, 2011; McCormick and Levin, 2017; Sato et al., 2018) to the community and ecosystem (Stramma et al., 2010; Doney et al., 2012; Matabos et al., 2012; Chu and Tunnicliffe, 2015a). As species vary in their tolerance to hypoxia (Vaquer-Sunyer and Duarte, 2008; Chu and Gale, 2017), they shape the spatiotemporal structuring of marine communities as oxygen content changes (Chu and Tunnicliffe, 2015a; Chu and Gale, 2017). Thus, ecosystems experiencing oxygen loss are valuable settings in which to test predictions of community disassembly.

A unique ecological monitoring program exists in Saanich Inlet, British Columbia, Canada – a fjord subject to yearly hypoxic events. Here, a continuous seafloor oxygen time-series from the VENUS cabled observatory ([www.oceannetworks.ca](http://www.oceannetworks.ca)) is coupled with near-annual remotely operated vehicle (ROV) visual surveys equipped with onboard oxygen sensors to monitor the effects of natural, but expanding, hypoxic events on epibenthic community structure (Chu and Tunnicliffe, 2015a). The first eight years (2006–2013) of these data characterized a gradual decline in both the benthic oxygen and the community, and serve as a benchmark for comparisons. Chu and Tunnicliffe (2015a) described the influence of the 2013 seasonal deoxygenation-reoxygenation cycle on the spatial reorganization of the epibenthic community. From 2015 to 2016, this system experienced a notable period of sustained, severe hypoxia (Gasbarro et al., 2017; Chu et al., 2018b) in which the mean oxygen levels dropped and remained below an ecophysiology-based hypoxia threshold established for this region (Chu and Gale, 2017). The hypoxic event coincided with a large warm temperature anomaly in the northeast Pacific ocean in 2014–15 (Bond et al., 2015) that was recorded in the Salish Sea during a notably strong El Niño in 2016 (Jacox et al., 2016; Ross, 2017). Here, by examining features of the species interaction network, we test the hypothesis that the prolonged 2015–2016 hypoxia event induced disassembly of the epibenthic megafaunal assemblage. We combine long-term bottom oxygen data from the VENUS observatory (2006–2017) with megafaunal abundance data from recent benthic ROV visual surveys to compare the community structure before (2013) and after (2016) the period of sustained, severe hypoxia. Our results provide novel insights into the disassembly effects of sustained exposure to a major marine climate stressor.

## 2. Materials & methods

### 2.1. Study site

Saanich Inlet has a maximum depth of 230 m and a shallow sill (75 m) at the mouth of the fjord that limits exchange with the adjacent Strait of Georgia. Seasonal hypoxia develops in mid-to-late summer as a result of the high primary productivity consumed at depth by microbial respiration (Herlinveaux, 1962; Grundle et al., 2009; Zaikova et al., 2010). Annual deep-water oxygen renewal occurs in the fall when dense, oxygenated water flows over the sill, descends into the bottom layers of the inlet, and displaces deoxygenated waters upward (Anderson and Devol, 1973; Tunnicliffe, 1981). A spring mid-depth (90–160 m) oxygen renewal can occur in some years (Manning et al., 2010; Pörtner, 2010). Although timing and extent of the depletion and renewal phases vary (Chu and Tunnicliffe, 2015a; Capelle et al., 2018), the seasonal phases of oxygen depletion and recovery are relatively predictable.

### 2.2. Long-term dissolved oxygen record

Since February 2006, the VENUS cabled subsea observatory of Ocean Networks Canada has measured dissolved oxygen concentration ( $[O_2]$ ) at one-minute intervals at our study site in Saanich Inlet (open data at [www.oceannetworks.ca](http://www.oceannetworks.ca)). VENUS instrumentation is located ~200 m south of the mid-point of our transect at 96 m depth, and captures the seasonal and long-term dynamics of  $[O_2]$  at about 1.5 m off-bottom. Following Chu and Tunnicliffe (2015a), we updated the 10-year VENUS  $[O_2]$  time-series to include the notable 2015–2016 hypoxia event and examined the trend over this period by averaging data from one-minute into one-hour intervals from April 2006 to April 2017. Time-series endpoints were chosen to ensure that oxygen levels were at roughly equivalent levels in order to control for the cyclical shape of the seasonal deoxygenation-reoxygenation. Data gaps (~7% of the time-series) were linearly interpolated prior to analyses. Annual  $[O_2]$  trends with respect to specific hypoxia thresholds were analyzed using a one-year running mean and annual means of VENUS time-series using the R packages 'xts' (Ryan and Ulrich, 2017) and 'zoo' (Zeileis and Grothendieck, 2017). Because the choice of oxygen units is discipline-specific (Rabalais et al., 2010; Pörtner, 2010), we report  $[O_2]$  in both  $mL L^{-1}$  (the traditional unit in ecology) and the SI unit  $\mu mol kg^{-1}$  ( $1 mL L^{-1} = 43.6 \mu mol kg^{-1}$  based on the average site conditions of 9 °C, 31 PSU,  $1.025 kg L^{-1}$ ). All raw CTD and oxygen data are available for additional unit conversions (Chu and Tunnicliffe, 2015b, Dryad package). For this study we used two hypoxia thresholds: the first at  $[O_2] = 0.5 mL L^{-1}$  or  $21.8 \mu mol kg^{-1}$  severe hypoxia threshold associated with fish kills in surface waters of the northeast Pacific (Chan et al., 2008) and the second at  $0.88 mL L^{-1}$  or  $38.4 \mu mol kg^{-1}$  which is a regional threshold developed for the East Pacific calculated using a biogeographical meta-analysis of ecophysiological traits associated with hypoxia (Chu and Gale, 2017).

### 2.3. Remotely operated vehicle (ROV) transect & video analysis

The same soft-substratum, benthic ROV transect has been replicated on a near-annual basis in Patricia Bay, Saanich Inlet, B.C. since 2006 ( $n = 13$ , see Chu and Tunnicliffe, 2015a for survey design details). It climbs from 180 to 40 m over a lateral distance of ~2–3 km and transitions through a steep oxygen gradient ( $[O_2]$  range  $0\text{--}4.5 mL L^{-1}$  or  $0\text{--}196.2 \mu mol kg^{-1}$ ). An ROV-mounted Sea-Bird SBE 19plus v2 conductivity-temperature-depth (CTD) and an SBE43 oxygen electrode, with the intake ~0.5 m above the ROV bottom, enabled us to measure the habitat  $[O_2]$  levels associated with all animals encountered during the survey. The transect was flown three times in 2013 (i.e. spring, summer, and fall) to characterize the influence of seasonal expansion and contraction of the hypoxic waters on the epibenthic community

(Chu and Tunnicliffe, 2015a). Three transects were completed at approximately the same times of year in 2016. Because of logistic constraints, the fall 2016 transect was truncated at the deeper, anoxic end of the survey (start depth ~ 140 m), but still captured the full [O<sub>2</sub>] range that influences species distributions at this site.

Two ROVs (*ROPOS* and the *Oceanic Explorer*) executed this transect. Navigation data were recorded on all *ROPOS* transects with an ultrashort baseline system, while navigation data for *Oceanic Explorer*-flown transects were interpolated post hoc by matching georeferenced 5 m gridded multibeam bathymetry data with the CTD bottom depths recorded along the transect. We compared [O<sub>2</sub>] data from our fall 2016 ROV transect with all fall/winter transects (i.e. October–December) dating back to 2006 (data available from Chu and Tunnicliffe, 2015b) to examine inter-annual bottom [O<sub>2</sub>] renewals; all other analyses used only data from 2013 and 2016 transects. We noted the deepest occurrence of the slender sole, *Lyopsetta exilis*, as it was typically the first benthic animal to appear along the deep-to-shallow transit. As one of the most hypoxia-tolerant megafauna at this site (Chu and Tunnicliffe, 2015a), the maximum depth of occurrence correlates with the lower [O<sub>2</sub>] limit of megafaunal habitation.

Individual animals (> 2 cm) were identified and counted for each second of transect video, standardized by area of the video frame, and then pooled into 20 m<sup>2</sup> quadrats ( $n = 538, 367$  respectively for 2013, 2016) using sequential seconds of annotated video (Chu and Tunnicliffe, 2015a). A smaller field of view in transects flown with the ROV *Oceanic Explorer*, along with the truncation of the deeper, anoxic part of the fall 2016 transect account for the difference in total number of quadrats between years. Abundance data were compiled for all species for each of the three seasons in both 2013 and 2016. Density, along with mean and minimum [O<sub>2</sub>] occurrence, were calculated for an assemblage of 14 mobile species and a sessile species (sea whip *Halipteria willemoesti*) (Table 1). Species in this assemblage were representative of the range of interspecific differences in oxygen distributions spanning the spatial hypoxia gradient, and were selected

based on consistent presence across seasons/years up to the 2013 benchmark (Chu and Tunnicliffe, 2015a). In addition, this assemblage contains a mix of common (e.g. slender sole, sea whip) and rare (e.g. tanner crab *Chionoectes bairdi*, spiny pink star *Pisaster brevispinus*) species. CTD and [O<sub>2</sub>] data were averaged per quadrat and matched with the navigation and species data by synchronized timestamps prior to analysis in R (R Core Team, 2017).

#### 2.4. Community structure along the oxygen gradient

We first tested whether community segregation was influenced by changes in the oxygen regime by using a null model analysis to generate community co-occurrence scores (c-scores, Stone and Roberts, 1990) for each season in 2013 and 2016; presence-absences for the 14 mobile species (see Tables S1–S3) comprised the data for our null model analyses (see below). The c-score quantifies community segregation as the product of the number of sites (i.e. quadrats) in which each species occurs and the number of sites shared with the next species. Community-level segregation is determined from c-scores calculated among all species pairs. We calculated c-scores using the sim4 ‘fixed-proportional’ algorithm in the R package EcosimR (Gotelli et al., 2015), which preserves species totals in the original matrix and assigns probabilities to quadrats relative to the totals; this method preserves species-site heterogeneity and is conservative (i.e. has a relatively low Type I error rate when compared to other algorithms) in distinguishing non-randomness in the observed data matrices (Gotelli, 2000). The average covariance in association between species pairs (V-ratio; Schluter, 1984) was also calculated for each transect; V-ratios increase as communities become more aggregated, thus allowing us to examine whether species pairs segregated or co-occurred during the intense hypoxic event. In addition, the checker score, i.e. the number of species pairs that never co-occur, was calculated for each transect (Gotelli, 2000) in order to determine if the 2016 hypoxic event led to fewer species experiencing complete separation.

**Table 1**

Pairs (2013, 2016) of mean  $\pm$  2\*SE (per 20 m<sup>-2</sup> quadrat), minimum oxygen occurrence, and density for 14 abundant mobile megabenthos and sessile sea whip in each season.

| Species                | O <sub>2</sub> -mean Spring         | O <sub>2</sub> -mean Summer          | O <sub>2</sub> -mean Fall           | O <sub>2</sub> -min Spring | O <sub>2</sub> -min Summer | O <sub>2</sub> -min Fall | Density spring                       | Density summer                        | Density fall                         |
|------------------------|-------------------------------------|--------------------------------------|-------------------------------------|----------------------------|----------------------------|--------------------------|--------------------------------------|---------------------------------------|--------------------------------------|
| Slender sole           | 1.38 $\pm$ 0.07,<br>2.01 $\pm$ 0.17 | 1.02 $\pm$ 0.01,<br>0.87 $\pm$ 0.2   | 0.89 $\pm$ 0.03,<br>0.79 $\pm$ 0.11 | 0.03,<br>0.07              | 0.03,<br>0.02              | 0.00,<br>0.03            | 9.56 $\pm$ 0.43,<br>4.13 $\pm$ 0.45  | 9.48 $\pm$ 0.13,<br>7.25 $\pm$ 0.43   | 10.35 $\pm$ 0.40,<br>2.73 $\pm$ 0    |
| Bluebarred prickleback | 1.47 $\pm$ 0.14,<br>1.48 $\pm$ 0.88 | 1.04 $\pm$ 0.01,<br>0.88 $\pm$ 0.03  | 0.65 $\pm$ 0.03,<br>0.31 $\pm$ 0.08 | 0.54,<br>0.34              | 0.88,<br>0.63              | 0.52,<br>0.12            | 0.73 $\pm$ 0.11,<br>0.07 $\pm$ 0.17  | 0.60 $\pm$ 0.13,<br>0.44 $\pm$ 0.10   | 1.30 $\pm$ 0.40,<br>0.39 $\pm$ 0.31  |
| Snake prickleback      | 4.17 $\pm$ 0.47,<br>3.82 $\pm$ 0.18 | 1.17 $\pm$ 0.07,<br>1.80 $\pm$ 0.15  | 2.08 $\pm$ 0.11,<br>2.23 $\pm$ 0.15 | 2.15,<br>2.20              | 0.87,<br>0.83              | 1.29,<br>0.21            | 0.11 $\pm$ 0.10,<br>0.85 $\pm$ 0.28  | 0.45 $\pm$ 0.05,<br>0.26 $\pm$ 0.08   | 0.82 $\pm$ 0.16,<br>0.46 $\pm$ 0.10  |
| Blackbelly eelpout     | 2.95 $\pm$ 0.27,<br>2.88 $\pm$ 0.28 | 1.04 $\pm$ 0.02,<br>1.20 $\pm$ 0.08  | 1.31 $\pm$ 0.09,<br>1.37 $\pm$ 0.19 | 0.68,<br>0.93              | 0.69,<br>0.79              | 0.58,<br>1.27            | 0.56 $\pm$ 0.05,<br>0.39 $\pm$ 0.10  | 0.48 $\pm$ 0.03,<br>0.75 $\pm$ 0.09   | 0.76 $\pm$ 0.10,<br>0.02 $\pm$ 0.37  |
| Blacktip poacher       | 2.05 $\pm$ 0.28,<br>1.08 $\pm$ 0.21 | 1.15 $\pm$ 0.07,<br>0.93 $\pm$ 0.05  | 0.87 $\pm$ 0.09,<br>1.51 $\pm$ 0.37 | 0.90,<br>0.35              | 1.03,<br>0.80              | 0.52,<br>0.68            | 0.26 $\pm$ 0.07,<br>0.25 $\pm$ 0.43  | 0.28 $\pm$ 0.05,<br>0.43 $\pm$ 0.13   | 0.43 $\pm$ 0.07,<br>0.08 $\pm$ 0.16  |
| Plainfin midshipman    | na,<br>2.96 $\pm$ 1.13              | 1.22 $\pm$ 0.04,<br>1.34 $\pm$ 0.42  | 1.43 $\pm$ 0.18,<br>1.83 $\pm$ 0.59 | na,<br>0.97                | 1.14,<br>0.61              | 0.43,<br>0.73            | 0,<br>0.08 $\pm$ 0.11                | 0.04 $\pm$ 0.05,<br>0.05 $\pm$ 0.05   | 0.27 $\pm$ 0.06,<br>0.04 $\pm$ 0.12  |
| English sole           | 4.36 $\pm$ 0.22,<br>2.75 $\pm$ 0.61 | 1.01 $\pm$ 0.04,<br>1.70 $\pm$ 0.29  | 2.70 $\pm$ 0.38,<br>2.20 $\pm$ 0.24 | 3.61,<br>1.28              | 0.87,<br>0.81              | 1.37,<br>1.90            | 0.08 $\pm$ 0.06,<br>0.13 $\pm$ 0.09  | 0.17 $\pm$ 0.04,<br>0.14 $\pm$ 0.08   | 0.05 $\pm$ 0.07,<br>0.06 $\pm$ 0.18  |
| Squat lobster          | 1.01 $\pm$ 0.02,<br>2.01 $\pm$ 0.19 | 0.98 $\pm$ 0.01,<br>0.82 $\pm$ 0.004 | 0.56 $\pm$ 0.01,<br>0.41 $\pm$ 0.02 | 0.40,<br>0.25              | 0.54,<br>0.56              | 0.01,<br>0.21            | 10.27 $\pm$ 5.10,<br>9.36 $\pm$ 7.17 | 7.57 $\pm$ 0.25,<br>11.81 $\pm$ 1.01  | 14.25 $\pm$ 1.12,<br>8.33 $\pm$ 9.60 |
| Spot prawn             | 3.64 $\pm$ 0.10,<br>1.15 $\pm$ 0.03 | 1.05 $\pm$ 0.02,<br>1.55 $\pm$ 0.13  | 1.92 $\pm$ 0.07,<br>na              | 1.12,<br>0.79              | 0.87,<br>0.82              | 0.66,<br>na              | 3.73 $\pm$ 0.23,<br>4.48 $\pm$ 7.75  | 1.36 $\pm$ 0.12,<br>0.69 $\pm$ 0.15   | 4.56 $\pm$ 0.39,<br>0                |
| Pink shrimp            | 4.01 $\pm$ 0.41,<br>1.28 $\pm$ 0.33 | 1.14 $\pm$ 0.01,<br>1.41 $\pm$ 0.34  | 1.25 $\pm$ 0.02,<br>na              | 1.22,<br>0.88              | 1.01,<br>0.81              | 0.60,<br>na              | 0.49 $\pm$ 0.57,<br>0.20 $\pm$ 0.31  | 5.60 $\pm$ 0.52,<br>0.13 $\pm$ 0.07   | 4.75 $\pm$ 1.78,<br>0                |
| Humpback shrimp        | 2.46 $\pm$ 0.23,<br>1.02 $\pm$ 0.19 | 1.20 $\pm$ 0.05,<br>2.12 $\pm$ 0.06  | 2.67 $\pm$ 0.04,<br>na              | 2.31,<br>0.90              | 0.92,<br>2.09              | 1.40,<br>na              | 0.14 $\pm$ 1.02,<br>0.06 $\pm$ 0.45  | 0.33 $\pm$ 0.09,<br>0.02 $\pm$ 0.17   | 1.12 $\pm$ 1.24,<br>0                |
| Dungeness crab         | 3.37 $\pm$ 0.67,<br>3.72 $\pm$ 0.94 | 1.26 $\pm$ 0.21,<br>2.03 $\pm$ 0.26  | 1.73 $\pm$ 0.57,<br>2.42 $\pm$ 0.10 | 2.44,<br>1.16              | 0.90,<br>0.96              | 1.26,<br>2.35            | 0.03 $\pm$ 0.10,<br>0.08 $\pm$ 0.11  | 0.08 $\pm$ 0.04,<br>0.08 $\pm$ 0.05   | 0.03 $\pm$ 0.11,<br>0.03 $\pm$ 0.09  |
| Tanner crab            | 2.94 $\pm$ 1.04,<br>4.38 $\pm$ 0.13 | 1.05 $\pm$ 0.14,<br>1.89 $\pm$ 0.16  | 1.74 $\pm$ 0.21,<br>2.35 $\pm$ 0.73 | 2.32,<br>4.24              | 0.87,<br>1.50              | 1.30,<br>1.98            | 0.02 $\pm$ 0.09,<br>0.04 $\pm$ 0.24  | 0.03 $\pm$ 0.05,<br>0.12 $\pm$ 0.11   | 0.10 $\pm$ 0.10,<br>0.02 $\pm$ 0.13  |
| Spiny pink star        | 4.56 $\pm$ 0.11,<br>na              | 1.90 $\pm$ 0.23,<br>2.31             | 2.29 $\pm$ 0.48,<br>2.74 $\pm$ 0.04 | 4.41,<br>na                | 1.11,<br>2.31              | 0.70,<br>2.68            | 0.03 $\pm$ 0.08,<br>0                | 0.06 $\pm$ 0.08,<br>0.01 $\pm$ 0.16   | 0.07 $\pm$ 0.09,<br>0.03 $\pm$ 0.15  |
| Sea whip               | 4.13 $\pm$ 0.05,<br>3.83 $\pm$ 0.05 | 1.26 $\pm$ 0.04,<br>2.00 $\pm$ 0.02  | 2.52 $\pm$ 0.04,<br>2.03 $\pm$ 0.08 | 1.79,<br>2.48              | 0.87,<br>0.96              | 1.22,<br>0.21            | 13.99 $\pm$ 1.18,<br>5.78 $\pm$ 1.27 | 11.98 $\pm$ 1.03,<br>10.20 $\pm$ 1.73 | 26.26 $\pm$ 3.59,<br>2.61 $\pm$ 0.46 |

Next, we examined changes in pairwise species associations ( $n = 91$ ) among the 14 mobile species between 2013 and 2016 using the FORTRAN program 'Pairs' (Ulrich, 2008). Null model simulations ( $n = 100$ ) based on observed presence-absence distributions were used to test whether a given species pair co-occurred more or less than expected from an empirical Bayesian distribution. Transformed z-scores (Observed - Expected/St. Dev.) with a false-error rate correction (Benjamini and Yekutieli, 2001) were calculated for species pairs with observed frequencies above or below the null expectation. We note that for species pairs that never occur together, the algorithm does not detect a significant deviation from null model expectations.

Finally, we tested for breaks in community structure using a multivariate regression tree (MRT; De'ath, 2002). MRT is a constrained ordination method where terminal leaves of the tree represent community types characterized by multispecies abundance data. Predictor variables constrain where breaks occur by minimizing within-groups sum of squares. Abundance data (ind.  $20\text{ m}^{-2}$ ) for the 14 mobile species were 4th-root transformed prior to MRT analysis in order to incorporate contributions from the rarer taxa (e.g. tanner crab) without eliminating the signal from the most abundant species (e.g. slender sole). We used normalised (mean = 0 and unit variance) environmental data including dissolved oxygen, temperature, salinity, and depth as predictor variables along with year.

### 3. Results

#### 3.1. Long-term oxygen trend from the VENUS time-series (2006–2016)

From 2006 to 2016, hourly dissolved oxygen concentration ( $[\text{O}_2]$ ) measured at the 96 m VENUS observatory declined at a rate of  $0.07\text{ mL L}^{-1}\text{ year}^{-1}$  or  $3.1\text{ }\mu\text{mol kg}^{-1}\text{ year}^{-1}$  ( $y = 1.48\text{ mL L}^{-1}$ ,  $r^2 = 0.11$ ,  $p < 0.001$ ), which is an increase from the rate of  $0.05\text{ mL L}^{-1}$  or  $2.2\text{ }\mu\text{mol kg}^{-1}\text{ year}^{-1}$  reported for the first eight years of the time-series (Chu and Tunnicliffe, 2015a). The updated VENUS time-series suggest this accelerated rate of oxygen decline is a result of the recent anomalous events (2015–2016). The annual  $[\text{O}_2]$  maximum did not exceed  $3\text{ mL L}^{-1}$  or  $131\text{ }\mu\text{mol kg}^{-1}$  in either 2015 or 2016, which was the first record of consecutive years at such low levels (Fig. 1a). Anoxia developed in mid-September and persisted to the

following January in both 2015 and 2016. In contrast, seasonal anoxia at 96 m only occurred once in the VENUS time-series from 2006 to 2014 (mid-October 2012 to early January 2013). A one-year running mean applied to the per minute  $[\text{O}_2]$  data also shows a general decline over the 10-year period with the annual mean  $[\text{O}_2]$  falling below the severe hypoxia threshold in 2015 (Fig. 1b). Finally, the annual  $[\text{O}_2]$  mean also fell below this threshold for the first time in 2015 and, in 2016, stayed below the  $0.88\text{ mL L}^{-1}$  or  $38\text{ }\mu\text{mol kg}^{-1}$  East Pacific hypoxic threshold (Fig. 1c).

#### 3.2. ROV oxygen profiles

Along-bottom  $[\text{O}_2]$  profiles differed notably between 2013 and 2016 with hypoxia and severe hypoxia extending shallower in all seasons of 2016; hypoxic and anoxic waters expanded over the course of the summer leading to the greatest recorded reduction of aerobically viable habitat for megafauna in fall 2016. The maximum depth of occurrence for slender sole was shallower in each season compared to 2013 (Fig. 2a, b). Again, the difference between 2013 and 2016 was most notable between the fall transects, where the deepest slender sole occurred at  $\sim 155\text{ m}$  in 2013 versus  $\sim 95\text{ m}$  in 2016. The 2016 profiles, particularly spring and fall, had sharp boundaries between hypoxia and normoxia, while  $[\text{O}_2]$  increased more gradually with decreasing depth in 2013 (Fig. 2a, b); a smaller proportion of the habitat surveyed in 2016 transects experienced  $[\text{O}_2]$  between  $1.1$  and  $1.8\text{ mL L}^{-1}$  (Fig. 2). In 2016, anoxia, severe hypoxia, and hypoxia expanded further into shallow depths compared to prior fall/winter transects (Fig. 2c). Among all fall transects in the ROV time-series, anoxia extended 40 m shallower in 2016 and covered 59% of the transect compared to 2013 where anoxia covered 31% and reached a minimum depth of  $\sim 133\text{ m}$ . While the extent of hypoxia decreased and the area of well-oxygenated habitat increased post-summer in 2013, this pattern was less apparent in 2016.

#### 3.3. 2013 vs. 2016 assemblage structure

We observed a 58% decrease in the total abundance of 46 species in our three surveys in 2016 ( $n = 10,718$  counts) relative to the similar surveys done in 2013 by Chu and Tunnicliffe (2015a). The effects of the

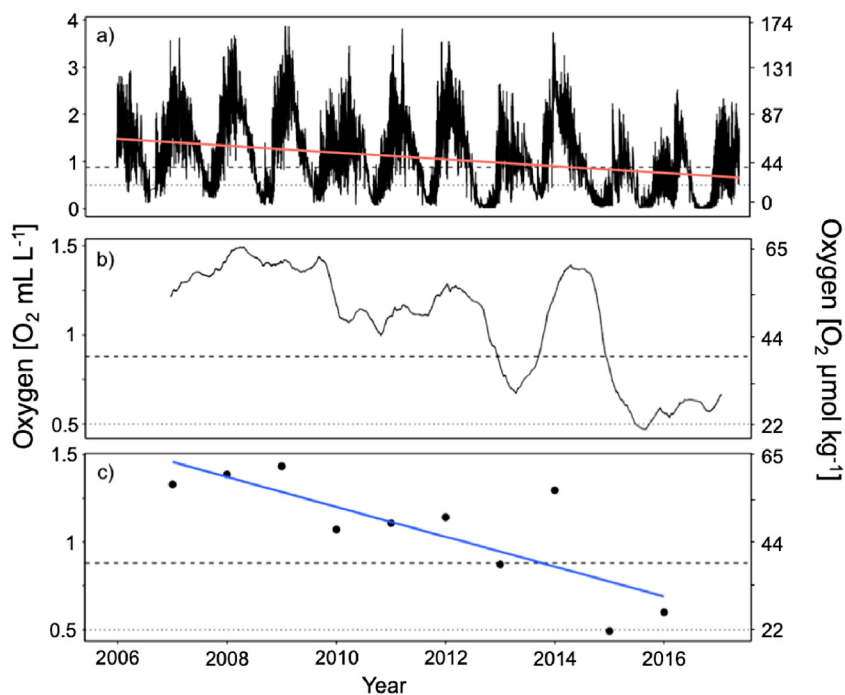


**Fig. 1.** Long-term (Apr 2006 to Apr 2017) dissolved oxygen ( $[\text{O}_2]$ ) trends from VENUS at 95 m.

(a) A regression line through the hourly average  $[\text{O}_2]$  data shows a decade-long decline in  $[\text{O}_2]$ , decreasing seasonal amplitude in the hypoxia cycle, and extended periods of anoxia in 2015–2016.

(b) A one-year running mean through the same data shows  $[\text{O}_2]$  drops below two hypoxia thresholds in 2015:  $[\text{O}_2] < 0.5\text{ mL L}^{-1}$  or  $22\text{ }\mu\text{mol kg}^{-1}$  (dotted line) and  $[\text{O}_2] < 0.88\text{ mL L}^{-1}$  or  $38\text{ }\mu\text{mol kg}^{-1}$  (dashed line). It remained below the latter threshold through to 2017.

(c) Annual mean  $[\text{O}_2]$  also fell below the severe hypoxia threshold in 2015, and was below this threshold through to 2016. A regression through the annual mean  $[\text{O}_2]$  (blue line) shows a consistent decline in  $[\text{O}_2]$  dating to 2007.

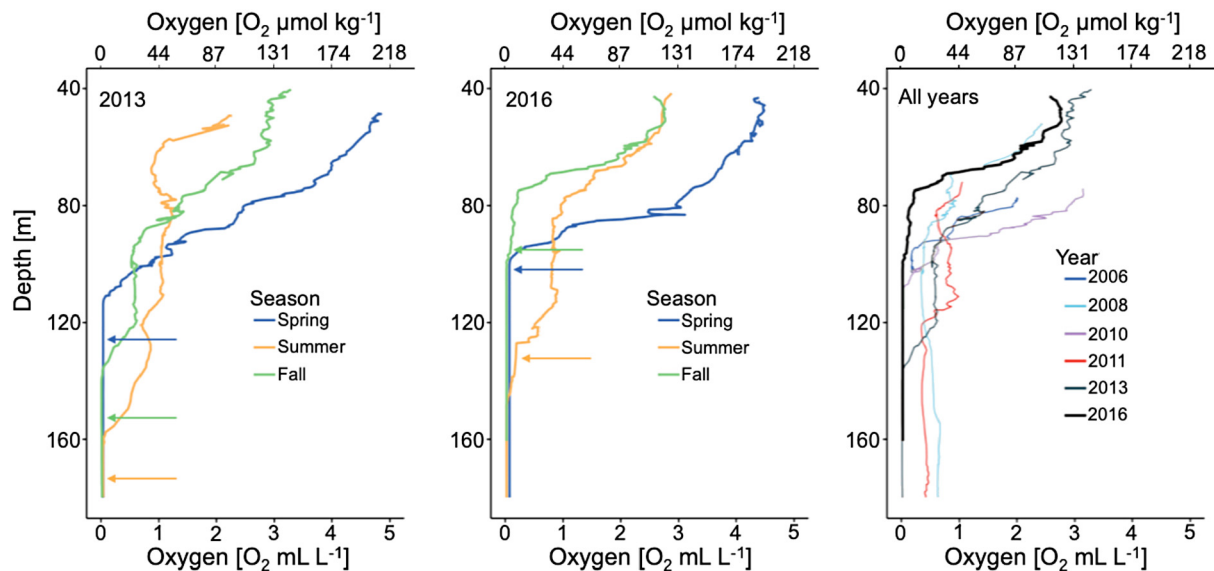


Fig. 2. Along-bottom oxygen ( $[O_2]$ ) profiles from ROV transects. Arrows show the deepest occurrence of slender sole (*L. exilis*) in each transect, representing the lower depth limit of megafauna and the shoaling of oxygenated habitat from summer to fall. Data are smoothed from per second  $[O_2]$  by averaging to 30-second intervals.

Profiles from (left) 2013 transects, (middle) 2016 transects, and (right) all Fall-Winter (Sep-Dec) transects completed since 2006.

In 2016, the depths of occurrence for anoxia, severe hypoxia ( $[O_2] < 0.5 \text{ mL L}^{-1}$  or  $22 \mu\text{mol kg}^{-1}$ ), and hypoxia ( $[O_2] < 0.88 \text{ mL L}^{-1}$  or  $38 \mu\text{mol kg}^{-1}$ ) thresholds are shallowest on record relative to previous surveys (2007–2013).

increase in spatiotemporal coverage of hypoxia varied by species with hypoxia-tolerant species displaying the weakest responses from 2013 to 2016. In addition to reduced overall numbers, populations generally occurred in lower oxygen in 2016 (Fig. 3), with notable increases in the number of organisms experiencing severe hypoxia in all seasons (Table 1). Densities of slender sole and squat lobster *Munida quadrispina*, were largely unchanged in the spring and summer seasons (Fig. 4), with the exception of a dense cluster of squat lobsters in spring 2016 that may have been a mating aggregation (Doya et al., 2016). However, both species declined in abundance and occurred at comparatively low  $[O_2]$  in fall 2016 when the volume of hypoxic waters was greatest. The sea whip, historically the most abundant animal on the transect (Chu and Tunnicliffe, 2015a), declined greatly in fall 2016 and experienced  $[O_2]$  as low as  $0.21 \text{ mL L}^{-1}$ ; in fall 2013 sea whips were not observed at  $[O_2]$  below  $1.22 \text{ mL L}^{-1}$  (Table 1). We observed many freshly fallen sea whips with soft tissue still visible. The spot prawn *Pandalus platyceros* occupied a low and narrow range ( $0.81\text{--}1.94 \text{ mL L}^{-1}$ ) of  $[O_2]$  in spring 2016 relative to spring 2013, and densities were low in summer 2016. The fall 2016 transect was also the first in the 10 years of this survey that spot prawn were completely absent. Two other pandalid shrimp, pink shrimp *P. jordani* and humpback shrimp *P. hypsinotus*, were absent in fall 2016, whereas at least two of these three species were present in every survey from 2006 to 2013 (Chu and Tunnicliffe, 2015a).

In addition to the marked decline in the shrimp populations, two species appeared in abundance that were never observed from 2006 to 2013. The striped nudibranch, *Armina californica*, was notably abundant in the shallow well-oxygenated segments of the summer ( $n = 68$ ) and fall ( $n = 167$ ) 2016 transects usually occupied by spot prawns. In addition, a high abundance of the burrowing white sea cucumber, *Pentamera calcigera* ( $n = 63$ ), emerged onto the sediment surface in fall 2016 and occupied a narrow range of low  $[O_2]$  ( $0.12\text{--}0.2 \text{ mL L}^{-1}$ ).

Oxygen values are presented in  $\text{mL L}^{-1}$  ( $1 \text{ mL L}^{-1} = 44 \mu\text{mol kg}^{-1}$ ). Both the observed and expected c-scores, reflecting the extent of segregation within the 14-species mobile assemblage, were higher in fall 2013 than 2016 transects (Table 2). C-scores were higher than expected from null model 95% CI in all seasons in 2013, but not significantly different from null in any 2016 transect. In both years, the degree of

community segregation fluctuated by season with the highest scores coming during the summer. The most notable difference in absolute c-scores between seasons in 2013 and 2016 occurred in the fall, where the c-score was 50.79 ( $p = 0.004$ ) in 2013 and 8.44 ( $p > 0.05$ ) in 2016. Average V-ratios that reflect species-pair associations (Table 2) were higher in spring and summer 2016 than the same seasons in 2013, suggesting aggregation; however, the V-ratio decreased in fall 2016 as abundances declined. Checker scores also declined in 2016 (Table 2) as more species infrequently co-occurred in a new, albeit diminished, habitat space as their numbers declined.

PAIRS analysis shows that, in the spring and summer seasons, species pairs were less likely to co-occur in 2013 than 2016; this pattern changed in the fall, when more species rarely or never co-occurred in 2016 (Fig. 5). The number of species with moderate co-occurrence scores ( $0.325\text{--}0.675$ ) also decreased in fall 2016, with the majority of species falling into the aggregated or segregated categories.

The numbers of species pairs with both significant positive and negative z-scores were lower in all seasons in 2016 than 2013. In 2013, the total number of associated pairs (segregated or aggregated) increased throughout the year, while in 2016 both significantly aggregated and segregated pairs peaked in the summer transects (Fig. 6d, e). Individual pairwise z-scores also differed between 2013 and 2016. Not all species pairs changed, however (Tables S1–S3). Of the notable changes, spot prawn and squat lobster went from significantly segregated in all seasons in 2013 to non-associated in spring 2016 and a relatively weak significant segregation (positive z-score) in summer 2016 (Fig. 6a). Two species pairs – slender sole/snake prickleback *Lumpenus sagitta* and blue-barred prickleback *Plectobranthus evides*/snake prickleback – also showed positive z-scores in summer and fall 2013, but their association was non-significant in all 2016 transects (Fig. 6b, c). There were zero or very few significantly aggregated or segregated pairs in both spring and fall 2016; in both these transects the number of significantly associated species-pairs did not rise above the 4.55 pairs expected at a 5% false detection rate. In total, the segregated pairs made up 57% of the significant associations in 2013 versus 64% in 2016. The lower number of both absolute associations and the higher proportion of segregated pairs in 2016 transects was driven in large part by decapod crustaceans ( $n = 6$  of 14 species); the rarity of these species

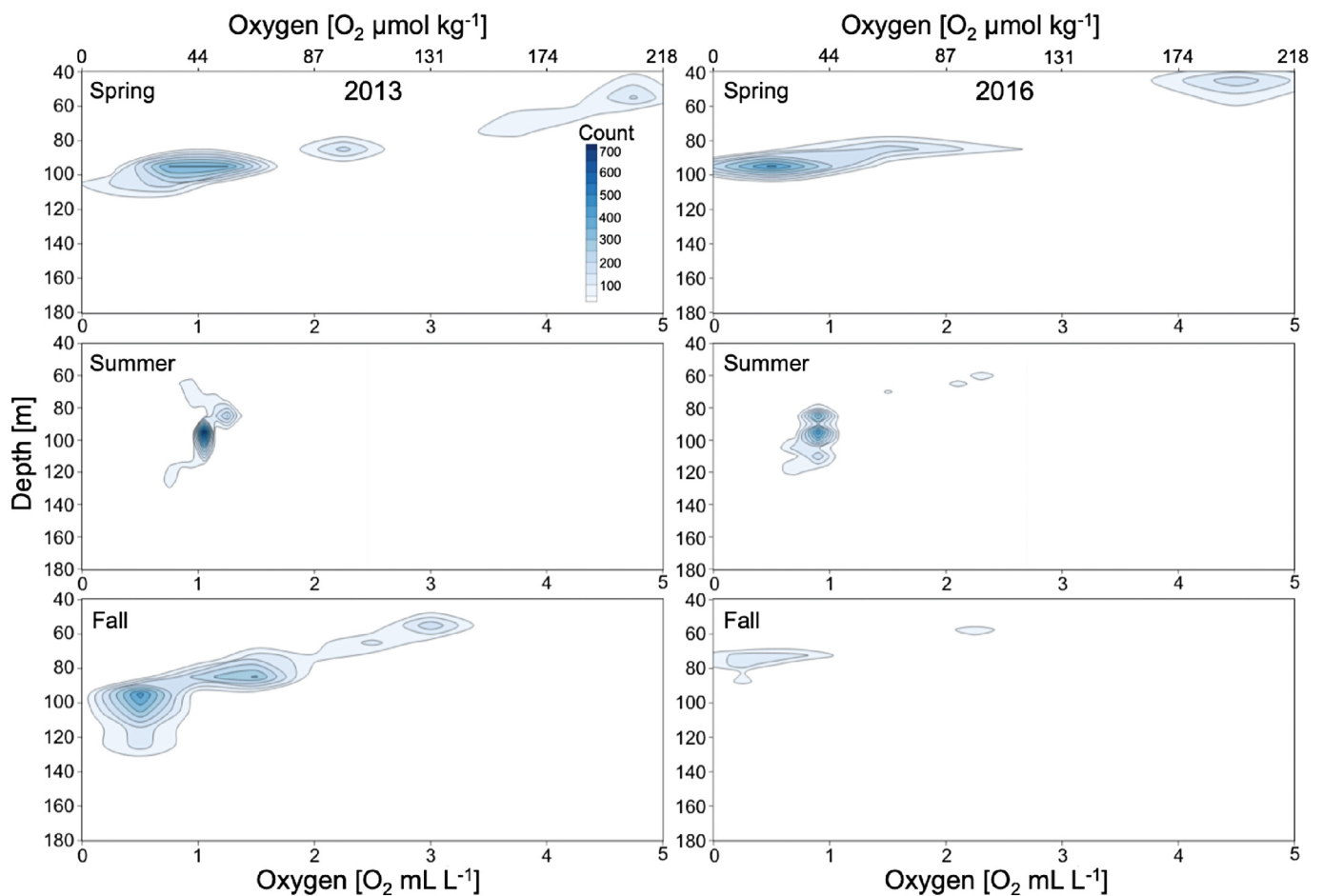


**Fig. 3.** Contour plots illustrate the distribution of megafaunal abundance (counts per  $20\text{ m}^{-2}$  quadrat) for all 46 species relative to depth and dissolved oxygen ( $[\text{O}_2]$ ) in 2013 and 2016. Overall abundance was lower in all seasons in 2016 compared to 2013.

**Depth:** Compared to 2013, peak abundances in 2016 shoaled and were constricted within a narrower  $[\text{O}_2]$  range. In 2016, loss of oxygenated habitat began in summer (shallower by 10 m) and was greatest in the fall (shallower by 25 m).

**Oxygen:** Abundance peaks also occur at lower  $[\text{O}_2]$  in spring ( $0.75\text{--}1.25\text{ mL L}^{-1}$  in 2013;  $0.5\text{ mL L}^{-1}$  in 2016), summer ( $1.05\text{ mL L}^{-1}$  in 2013;  $0.9\text{ mL L}^{-1}$  in 2016), and most notably in fall ( $0.5\text{--}1.5\text{ mL L}^{-1}$  in 2013;  $0.25\text{--}0.75\text{ mL L}^{-1}$  in 2016).

in 2016 transects may have limited the ability of the randomization algorithm to detect significant associations with other species when present. See Tables S1–S3 for PAIRS z-scores for all species combinations in each 2013 and 2016 transect season. Fig. 7 is a representation of the changes in species associations that occurred in Saanich Inlet over the course of this study.

### 3.4. Community structure thresholds

Multivariate regression tree (MRT) analysis (Fig. 8) revealed factors driving five transition points within the community ( $R^2 = 0.38$ ). When  $[\text{O}_2]$  is under  $1.8\text{ mL L}^{-1}$  ( $79\text{ }\mu\text{mol kg}^{-1}$ ), oxygen was the primary driver as different assemblages emerged at  $[\text{O}_2]$  thresholds of  $0.19$  ( $8\text{ }\mu\text{mol kg}^{-1}$ ),  $1.12\text{ mL L}^{-1}$  ( $49\text{ }\mu\text{mol kg}^{-1}$ ), and  $0.87\text{ mL L}^{-1}$  ( $37.9\text{ }\mu\text{mol kg}^{-1}$ ). The assemblage characterized by  $[\text{O}_2] < 0.19\text{ mL L}^{-1}$  ( $8.3\text{ }\mu\text{mol kg}^{-1}$ ) had the most quadrats ( $n = 339$ ), and was composed only of low densities of slender sole, squat lobster and bluebarred prickleback; thus, this leaf represents a severely hypoxic range tolerated by only three species. In the  $[\text{O}_2]$  range between  $0.19$  and  $0.87\text{ mL L}^{-1}$ , the abundances of slender sole and squat lobster drove assemblage structure which transitioned to include spot prawn, blackbelly eelpout *Lycodes pacificus*, and pink shrimp in the  $[\text{O}_2]$  range between  $0.87$  and  $1.12\text{ mL L}^{-1}$ . In the  $[\text{O}_2]$  range between  $1.12$  and  $1.8\text{ mL L}^{-1}$ , squat lobster were less abundant, while slender sole, spot prawn, and pink shrimp defined the assemblage structure; all species

were present in this range despite this leaf of the MRT containing the fewest quadrats ( $n = 78$ ). Squat lobster and pink shrimp were uncommon in the relatively higher end of the oxygen gradient ( $[\text{O}_2] > 1.8\text{ mL L}^{-1}$ ), while slender sole and spot prawn still occurred in high abundances. In higher  $[\text{O}_2]$  conditions, a temperature threshold at  $8.65\text{ }^\circ\text{C}$  explained an additional transition point in the community; high spot prawn and slender sole abundances in the shallow portions of two relatively cool 2013 transects contributed to this threshold. Season, year, and depth did not contribute to the creation of the most parsimonious MRT.

## 4. Discussion

Our novel time-series generated from recurring seafloor surveys allowed us to detect community disassembly caused by intense stress. The severity of the sustained 2015–2016 hypoxic event was evident in both the long-term observatory record and the induced biological response: we observed abundance declines and local extirpations in taxa sensitive to low oxygen, the emergence and proliferation of two species not recorded in the previous eight years prior to the sustained hypoxia event (Chu and Tunnicliffe, 2015a), compression of depth distributions when habitat was lost to shoaling hypoxia, and changes in species associations as abundances decreased. Spatial resorting of species occurs during deoxygenation because populations live near their lower, physiological limits to hypoxia (Seibel, 2011; Chu and Gale, 2017; Wishner

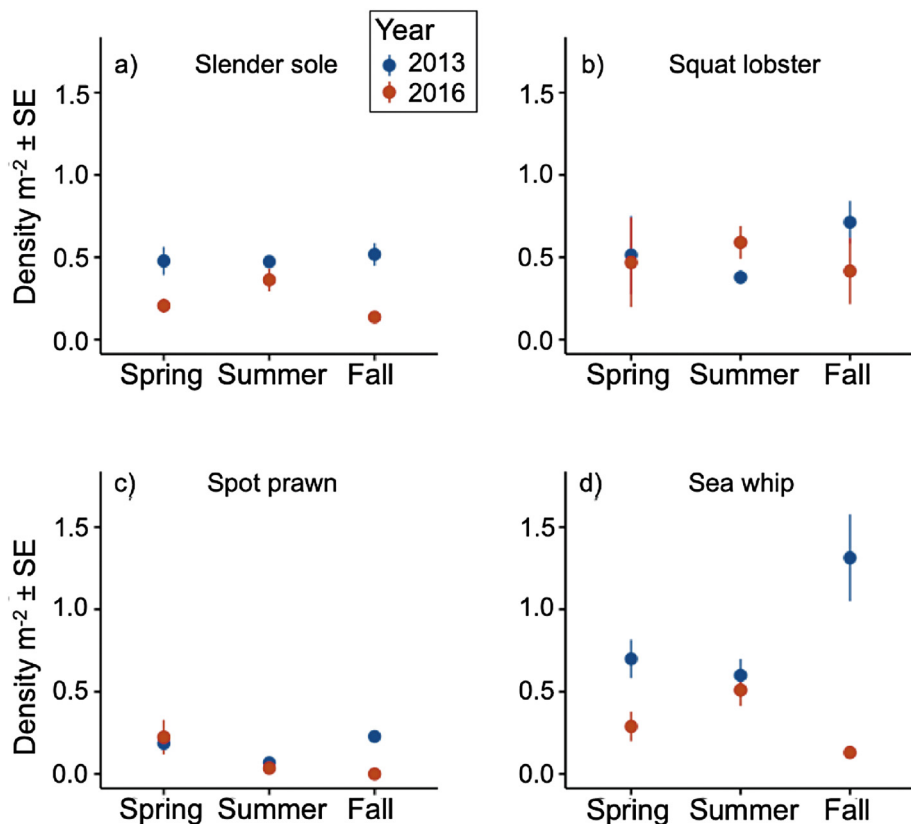


Fig. 4. Mean density (counts  $m^{-2} \pm SE$ ) of four key species in 2013 and 2016 transects. The density of hypoxia-tolerant slender sole and squat lobster declined less than spot prawn and sea whip. For the first time in this annually occurring survey, spot prawn were absent in the fall 2016 survey. Sea whip also experienced a notable 92.3% decline ( $n = 3939$  in 2013,  $n = 303$  in 2016).

(a) Slender sole *L. exilis*, (b) squat lobster *M. quadrispina*, (c) spot prawn *P. platyceros*, (d) sessile sea whip *H. willemoesi*.

Table 2

Mean simulated and observed community co-occurrence scores (c-scores) and their associated p-values and standard effect sizes (SES) for each 2013 and 2016 transect from null model analysis of species presence in  $20 m^{-2}$  quadrats. C-scores were significantly greater than null model expectation for 2013 data indicating a segregated community; no significant C-scores in 2016 data indicates a loss of community structure. The average covariance between species pairs (V-ratio) was lowest in fall 2016. Lower checker scores in 2016 (# of species-pairs that never co-occur) indicate more species are interacting in the latter year despite overall lower abundances.

|            | Mean simulated c-score | Observed c-score | p-Value | SES  | V-ratio | Checker score |
|------------|------------------------|------------------|---------|------|---------|---------------|
| Spring '13 | 43.10                  | 50.79            | 0.004   | 2.36 | 3.64    | 20            |
| Summer '13 | 61.90                  | 69.10            | 0.035   | 1.75 | 2.59    | 21            |
| Fall '13   | 43.26                  | 50.79            | 0.007   | 2.39 | 3.64    | 20            |
| Spring '16 | 17.50                  | 16.23            | > 0.05  | -    | 4.23    | 12            |
| Summer '16 | 20.85                  | 23               | > 0.05  | -    | 3.93    | 19            |
| Fall '16   | 9.15                   | 8.44             | > 0.05  | -    | 2.45    | 16            |

et al., 2018). Thus, when deoxygenation decreases the metabolic viability of benthic habitats, alterations to species abundances, distributions, and interactions will follow by compression of realized niche space (Stramma et al., 2012; Sato et al., 2017).

4.1. Hypoxia-induced community disassembly

Offshore systems in oxygen minimum zones (OMZ) can display habitat compression as a result of shoaling hypoxia (Stramma et al., 2012; Sato et al., 2017) as do coastal fjord systems (Jørgensen, 1980; this study). We first observed a response to habitat compression in spring 2016 as the loss of species segregation in the community. However, in fall 2016, a distinct disassembly stage followed from habitat compression wherein both the overall community and individual species showed pronounced abundance declines (Fig. 7; Fig. S1). While

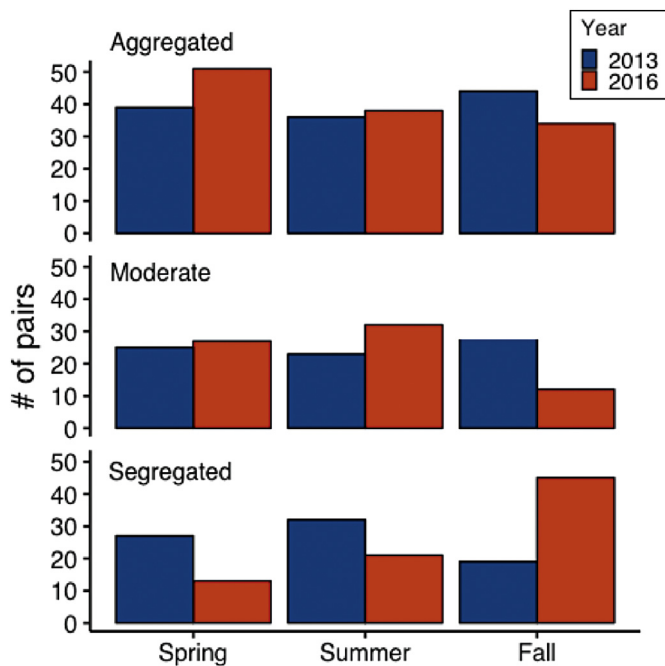


Fig. 5. Number of species pairs with co-occurrence scores in ranges of 0-0.325 (aggregated; top), 0.325-0.675 (moderate; middle) and 0.675-1 (segregated; bottom) in 2013 and 2016 transects. In spring and summer transects, more species were commonly or moderately aggregated in 2016 than in 2013. The increase in segregated species in fall 2016 is mostly accounted for by the number of pairs that never co-occurred due to abundance declines.

mobile species migrate to avoid transgressing their physiological limits to hypoxia (Craig and Crowder, 2005), this strategy becomes ineffective when the spatiotemporal extent of hypoxia exceeds their migratory

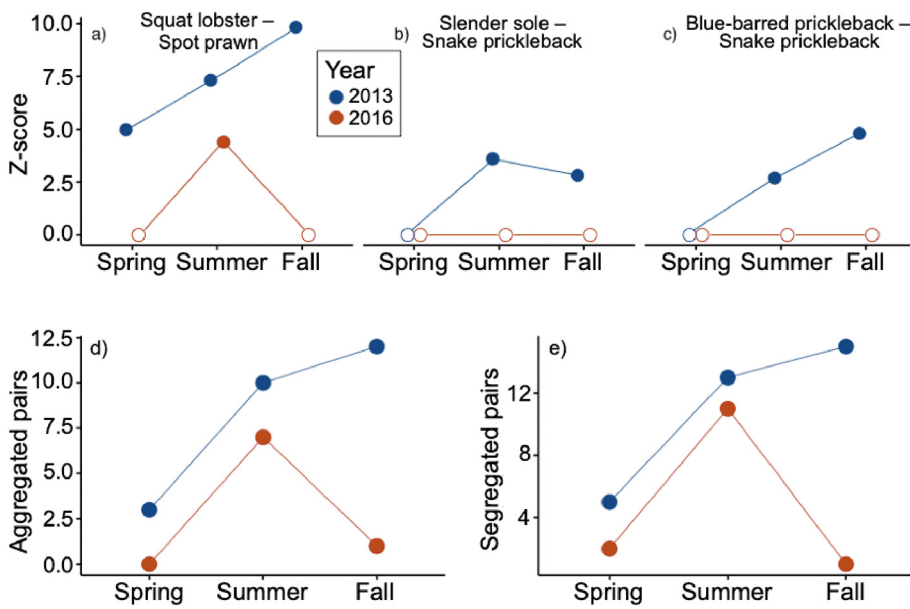


Fig. 6. Pairwise segregated associations from PAIRS analysis.

Notable examples of differences in Z-scores from 2013 to 2016 show significant associations (filled points) that diminish to become non-significant (hollow points) for: (a) squat lobster *M. quadrispina* - spot prawn *P. platyceros*, (b) slender sole *L. exilis* - snake prickleback *L. sagitta*, (c) blue-barred prickleback *P. evides* - snake prickleback. Other pairwise associations in the megabenthic assemblage are found in Tables S1–S3.

For analyses of all 14 megabenthic species: (d) total numbers of aggregated species pairs per transect in 2013 and 2016, and (e) total numbers of segregated species pairs per transect in 2013 and 2016.

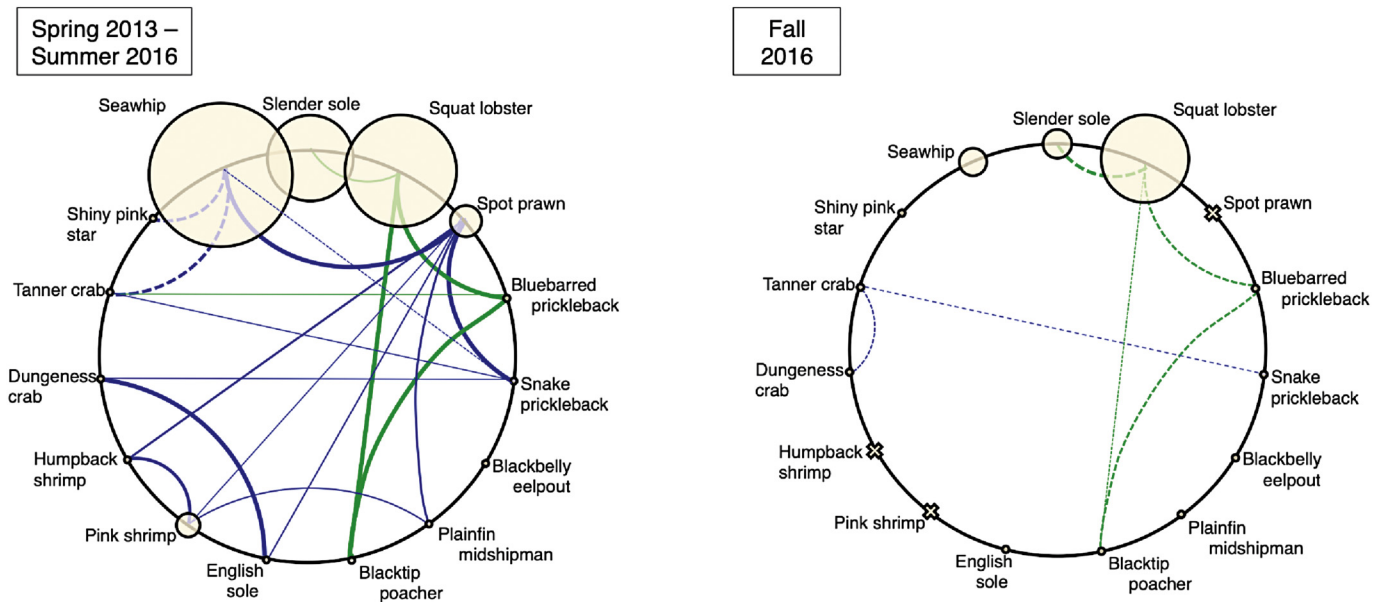
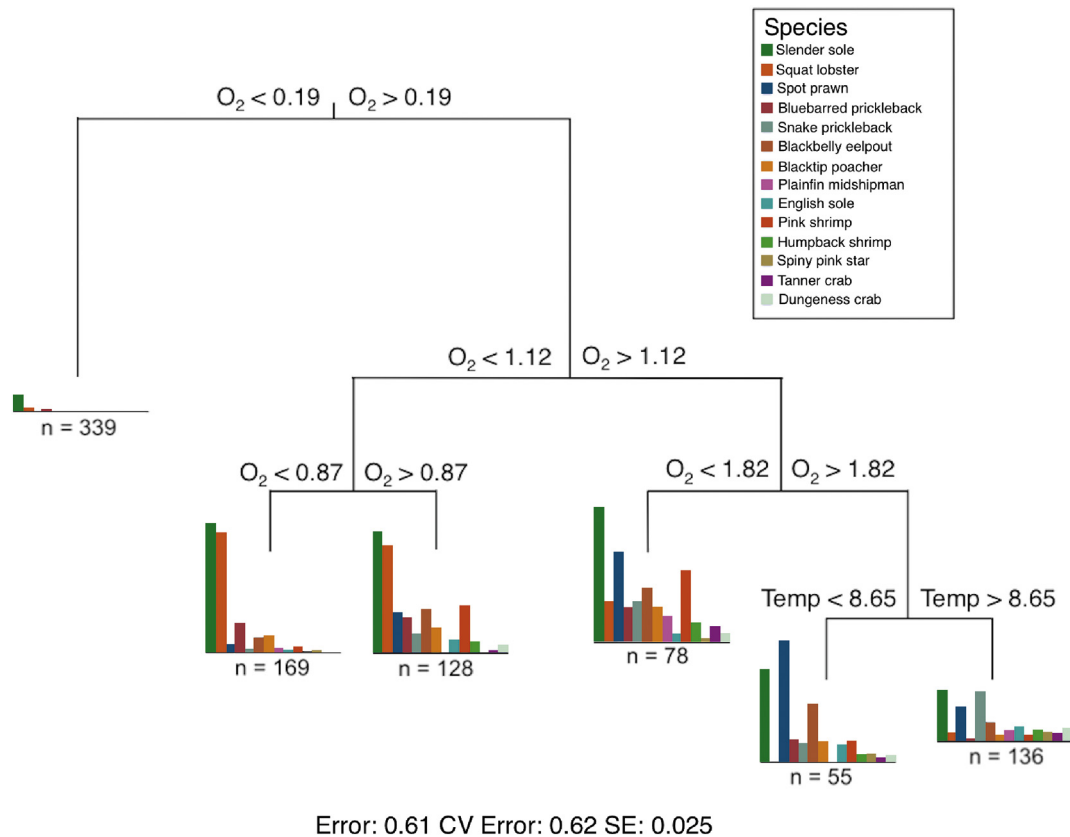


Fig. 7. Conceptual interaction networks before (left) and after (right) hypoxia-induced community disassembly in fall 2016. Networks consist of abundance-weighted nodes (species; circles) and interactions (lines) inferred from co-occurrences (Tables S1–S3), observations, and literature. Line thickness reflects frequency of aggregated pairs, while colors denote high-oxygen (blue) and low-oxygen (green) networks. Dashed lines are derived from observations, not PAIRS analysis; dotted lines are remaining observed (non-significant) associations. Fall 2016 extirpations are represented by crosses. Loss and decline of highly connected species (e.g. spot prawn and sea whip) in fall 2016 led to notably fewer species linkages and re-arranged community architecture. (For interpretation of the references to colour in this figure legend, the reader is referred to the web version of this article.)

abilities. A larger proportion of organisms experienced hypoxia in all seasons of 2016, indicating that hypoxia expansion had indeed outpaced avoidance strategies. Even populations of the most hypoxia-tolerant megafauna began to decline in fall 2016 as epibenthic community turnover was approaching a climax in late 2016.

We provide both direct and indirect evidence that the segregation of species niches, which enables species co-existence in a community (Amarasekare, 2003), was lost as a consequence of sustained hypoxia exposure. Several negative interactions likely occurred as a result of this forced overlap (Fig. 7). Resources that are generally partitioned along axes of energy and habitat availability (Ross, 1986; Chesson, 2000), likely diminished in fall 2016. The marked decline in species abundances would have caused declines in total food availability for the

benthic megafauna, potentially limiting niche diversity and the feasibility of multi-species niche packing (Mittelbach et al., 2001; McClain et al., 2018). Pandalid shrimp and squat lobster consume similar resources (Cartes, 1993; unpubl data) but usually occupy different areas in Saanich Inlet because of interspecific differences in hypoxia tolerance (Chu and Gale, 2017). Spot prawn appear to outcompete squat lobsters, potentially furthering segregation through negative interaction (i.e. resource competition; Anderson & Bell 2014). In 2016, they were forced into overlapping habitats; the additional stress of competition may have contributed to population declines. Forced overlap also occurred between squat lobsters and their predator the Dungeness crab, *Metacarcinus magister* (Tunncliffe, personal observation). In addition, the widespread and long-lasting hypoxia may have altered foraging



**Fig. 8.** Transitions in assemblage community structure identified using multivariate regression tree analysis. Species abundances combine data from 2013 and 2016 ( $n = 902$ ,  $20 \text{ m}^{-2}$  quadrats). Primary explanatory variables driving assemblage transition points in the tree are shown at each split. Mobile megabenthic species abundances (bar plots), primary explanatory variable values and the number of quadrats are displayed at each leaf to describe the different assemblages. Year and season did not influence the most parsimonious tree (5 splits) which explained  $\sim 38\%$  (1 – CV Error) of the variance in community structure suggesting the increased duration and spatial extent of hypoxia was the primary driver of community disassembly observed in 2016.

behaviour through sensory impairment (Bell et al., 2003; McCormick and Levin, 2017), furthering niche overlap. As slender sole were forced further upslope, species previously segregated from them may have experienced additional disturbance from their sediment resuspension activity (Yahel et al., 2008). Loss of three-dimensional biogenic habitat as a consequence of sea whip mortality ( $\sim 90\%$  density decrease from fall 2013 to fall 2016) may have also hastened the disappearance of spot prawn and other decapods typically seen among sea whip population (Chu and Tunnicliffe, 2015a), and diminished a buffer against disassembly in habitat complexity (Emslie et al., 2014).

Two species were new records in this time-series. The appearance of striped nudibranchs was probably aided by the expansion of their food source in the sea whips felled from oxygen stress (Nybakken and McDonald, 1981). Additionally, relaxed competition due to the extirpation of shrimp may have led to the increase in nudibranchs. In fall 2016, the extended period of severe hypoxia in the deep portions of the transect likely forced the white sea cucumber from their burrows, where chemosynthetic bacterial mats indicated hydrogen sulfide build-up in the sediment (Sturdivant et al., 2012). Similarly, during anoxia in 2012, burrowing infauna emerged onto the sediment surface at the VENUS observatory site (Chu et al., 2018a). Thus, the declines in abundance we describe appear to extend to the infauna. Collectively, these shifts from infaunal to epifaunal modes may decrease subsurface bioturbation and lead to further changes in infaunal communities (Nilsson and Rosenberg, 2000; Danovaro et al., 2008).

#### 4.2. Assemblage transitions along the hypoxia gradient

The  $[\text{O}_2]$  thresholds that delineate assemblage transitions within the

community in this study match ecophysiological thresholds calculated for species that are adapted to the low oxygen waters in this region. For example, the lowest  $[\text{O}_2]$  species grouping (occurring  $< 0.19 \text{ mL L}^{-1}$ ) is below the critical oxygen tensions of the main species in that assemblage (i.e. squat lobster and slender sole; Chu and Gale, 2017); such tolerant species use severely stressed habitat as transients (Briggs et al., 2017). Sperling et al. (2016) found a similar  $[\text{O}_2]$  threshold ( $\sim 0.16 \text{ mL L}^{-1}$ ) for infaunal communities of the east Pacific and Arabian Sea. The assemblage transition point at  $[\text{O}_2]$  of  $0.87 \text{ mL L}^{-1}$  matches the threshold calculated from critical oxygen tensions of crustaceans from the east Pacific (Chu and Gale, 2017) in an analysis that included species from offshore oxygen minimum zones. Up-slope movements of spot prawn, and pink shrimp were noted to occur in the  $[\text{O}_2]$  range of  $1\text{--}1.15 \text{ mL L}^{-1}$  by Chu and Tunnicliffe (2015a), matching our  $1.12 \text{ mL L}^{-1}$  assemblage break that was driven by abundance changes in these species. Thus, Saanich Inlet may be a tractable system for studying the effects of shoaling oxygen minimum zones (OMZs) on higher-trophic-level communities as suggested for protozoa (Torres-Beltrán et al., 2017, 2018) and other microbes (Walsh et al., 2009). This opportunity is especially relevant given the high rate of OMZ expansion in the northeast Pacific (Whitney et al., 2007; Crawford and Pena, 2016).

The assemblage transition point at the highest  $[\text{O}_2]$  occurred at  $1.8 \text{ mL L}^{-1}$ , which is above noted hypoxia thresholds for some taxonomic groups (Vaquer-Sunyer and Duarte, 2008), but still within the range of megabenthic turnover thresholds seen in other hypoxic systems (Kodama et al., 2010; Pörtner, 2010). This ‘high-oxygen’ threshold may be caused by a convergence between assemblages in this zone – with increased overlap caused by diminished habitat space – facilitating

increased species turnover or co-occurrences. Some hypoxia-sensitive species in our assemblage and multiple taxonomic groups can have critical oxygen thresholds in this range (Whyte & Carswell 1982; Vaquer-Sunyer and Duarte, 2008). Because species live close to their physiological limits to hypoxia (Seibel, 2011; Chu and Gale, 2017), physiological thresholds of the abundant species will match closely with the community transition points along an oxygen gradient. An additional temperature-driven transition point occurred when  $[O_2]$  was relatively higher ( $> 1.8 \text{ mL L}^{-1}$ ). While hypoxia can interact with additional physiological stressors such as temperature (Deutsch et al., 2015), thermal variability is low in the deeper sections of Saanich Inlet (180–90 m; St. Dev.  $\leq 0.5^\circ\text{C}$ ; Chu and Tunnicliffe, 2015b) with a small annual temperature range measured at the 96 m VENUS observatory site (7.8–9°C; Chu et al., 2018a). The potential influence of temperature stress occurs in the shallower areas ( $< 90 \text{ m}$ ) corresponding to where  $[O_2]$  transitions out of hypoxic conditions and thermal variability is greater. Although  $[O_2]$  levels may no longer be physiologically limiting for most species, warming can cause physiological hypoxia to shift towards a higher  $[O_2]$  by increasing critical oxygen tensions (Deutsch et al., 2015), which, in turn, manifests as the additional community transition point in ‘normoxic’ conditions. Therefore, ‘thresholds’ for one physiological stressor need to be placed in the context of others (Sperling et al., 2016) while also factoring in historical, geographic, and life-history traits that play additional roles in determining the disassembly sequence and transition points (Belyea and Lancaster, 1999; Darling et al., 2013; Sato et al., 2018).

Long-term ecosystem stressors such as deoxygenation and intermittent extreme events overlain on this chronic stress are both projected to increase in intensity and frequency (Harris et al., 2018), with the potential to send biological systems over critical and often irreversible thresholds (Scheffer et al., 2009). Therefore, characterizing sequences of community disassembly in natural systems and developing general biological indicators (e.g. O’Neill, 2016) are necessary to anticipate such transitions. Long-term, ecological monitoring programs that combine fixed and mobile platforms can capture the spatio-temporal shifts in community structure that emerge quickly in response to extreme events such as the intense hypoxia we describe in our study. In many benthic ecosystems, rapid change may outpace the ability of many slow-growing organisms to respond (Moffitt et al., 2015). The speed at which a system will recover to its former structure will be limited by recruitment and slow-growth of the sessile fauna (Chu et al., 2018a).

Recovery of a community interaction network will also be constrained by its new architecture which was reconfigured by the stressor event. Turnover in such networks is expected mostly among rare species with few linkages (Olesen et al., 2008). However, in Saanich, we found notable declines (e.g. sea whip) and extirpations (e.g. spot prawn) of formerly abundant species suggesting constriction or loss of large, well-connected nodes in the network. These lost and weakened linkages indicate an increasingly fragmented community (Thébault and Fontaine, 2010) that may cause further instability in the system (Saavedra et al., 2008; Daskalov et al., 2017). Should extended low-oxygen events such as those seen in 2015–2016 become more frequent, hypoxia-induced disassembly will also become more common as the current rate of global deoxygenation continues (Ito et al., 2017). Extreme events such as marine heat waves (Frölicher and Laufkötter, 2018) that produced the unprecedented thermal anomaly in the Northeast Pacific in 2014–15 (Bond et al., 2015) will increase as climate change proceeds (Harris et al., 2018). Disruption of community structure will be a likely outcome of such events, portending notable and potentially irreversible losses of biodiversity and ecosystem functioning across a variety of marine ecosystems.

Supplementary data to this article can be found online at <https://doi.org/10.1016/j.jmarsys.2019.103184>.

## Acknowledgements

The authors extend gratitude to P. Macoun, R. Jenkins, G. Parker, C. Adams, I. Kulin, A. Sastri and S. Mihaly, and K. Douglas and staff at Oceans Network Canada-VENUS for their continued support of this time-series and open source data. A portion of the data used in this work was provided by ONC. We thank the Canadian Scientific Submersible Facility, Island Tug and Barge, and the captains and crews of the CCGS Tully for their support in the field. Thanks to S.K. Juniper, J. Baum, and A. Sastri for helpful comments on an early version of this manuscript, to J. Rose for technical assistance, and N. Brown for help with video annotation. This research is sponsored by the NSERC Canadian Healthy Oceans Network and its Partners: Department of Fisheries and Oceans Canada and INREST (representing the Port of Sept-Îles and City of Sept-Îles). The authors declare that they have no conflict of interest.

## References

- Albert R, Jeong H, Barabási A-L (2000) Error and attack tolerance of complex networks. *Nature* 406:378–382.
- Amarasekare, P., 2003. Competitive coexistence in spatially structured environments: a synthesis. *Ecol. Lett.* 6, 1109–1122.
- Anderson, J.J., Devol, A.H., 1973. Deep water renewal in Saanich Inlet, an intermittently anoxic basin. *Estuar. Coast. Mar. Sci.* 1, 1–10.
- Anderson, G.S., Bell, L.S., 2014. Deep coastal marine taphonomy: investigation into carcass decomposition in the Saanich Inlet, British Columbia using a baited camera. *PLOS ONE* 9, e110710.
- Bascompte, J., Stouffer, D.B., 2009. The assembly and disassembly of ecological networks. *Philos. Trans. R. Soc. Lond. Ser. B Biol. Sci.* 364, 1781–1787.
- Bell, G.W., Eggleston, D.B., Wolcott, T.G., 2003. Behavioral responses of free-ranging blue crabs to episodic hypoxia: I. Movement. *Mar. Ecol. Prog. Ser.* 259, 215–225.
- Belyea, L.R., Lancaster, J., 1999. Assembly rules within a contingent ecology. *Oikos* 86, 402–416.
- Benjamini, Y., Yekutieli, D., 2001. The control of the false discovery rate in multiple testing under dependency. *Ann. Stat.* 29, 1165–1188.
- Bond, N.A., Cronin, M.F., Freeland, H., Mantua, N., 2015. Causes and impacts of the 2014 warm anomaly in the NE Pacific. *Geophys. Res. Lett.* 42, 3414–3420.
- Briggs, K.B., Craig, J.K., Shivarudrappa, S., Richards, T.M., 2017. Macrobenthos and megabenthos responses to long-term, large-scale hypoxia on the Louisiana continental shelf. *Mar. Environ. Res.* 123, 38–52.
- Capelle, D.W., Hawley, A.K., Hallam, S.J., Tortell, P.D., 2018. A multi-year time-series of  $N_2O$  dynamics in a seasonally anoxic fjord: Saanich Inlet, British Columbia. *Limnol. Oceanogr.* 63, 524–539.
- Cardinale, B.J., Duffy, J.E., Gonzalez, A., Hooper, D.U., Perrings, C., Venail, P., Narwani, A., Mace, G.M., Tilman, D., Wardle, D.A., Kinzig, A.P., Daily, G.C., Loreau, M., Grace, J.B., Larigauderie, A., Srivastava, D.S., Naeem, S., 2012. Biodiversity loss and its impact on humanity. *486. Natur*, London, pp. 59–67.
- Cartes, J., 1993. Diets of deep-water pandalid shrimps on the western Mediterranean slope. *Mar. Ecol. Prog. Ser.* 96, 49–61.
- Chan, F., Barth, J.A., Lubchenko, J., Kirincich, A., Weeks, H., Peterson, W.T., Menge, B.A., 2008. Emergence of anoxia in the California current large marine ecosystem. *Science* 319 (920–920).
- Chapman, A.S.A., Tunnicliffe, V., Bates, A.E., 2018. Both rare and common species make unique contributions to functional diversity in an ecosystem unaffected by human activities. *Divers. Distrib.* 24, 568–578.
- Chase, J.M., 2003. Community assembly: when should history matter? *Oecologia* 136, 489–498.
- Chesson, P., 2000. Mechanisms of maintenance of species diversity. *Annu. Rev. Ecol. Syst.* 31, 343–366.
- Chu, J.W.F., Gale, K.S.P., 2017. Ecophysiological limits to aerobic metabolism in hypoxia determine epibenthic distributions and energy sequestration in the northeast Pacific ocean. *Limnol. Oceanogr.* 62, 59–74.
- Chu, J.W.F., Tunnicliffe, V., 2015a. Oxygen limitations on marine animal distributions and the collapse of epibenthic community structure during shoaling hypoxia. *Glob Change Biol* 21, 2989–3004.
- Chu, J.W.F., Tunnicliffe, V., 2015b. Data from: oxygen limitations on marine animal distributions and the collapse of epibenthic community structure during shoaling hypoxia. Dryad Digital Repository. <https://doi.org/10.5061/dryad.1p55v>.
- Chu, J.W.F., Curkan, C., Tunnicliffe, V., 2018a. Drivers of temporal beta diversity of a benthic community in a seasonally hypoxic fjord. *Roy Soc Open Sci* 5, 172284.
- Chu, J.W.F., Gasbarro, R., Tunnicliffe, V., 2018b. The Saanich Inlet ROV transect 2017: Delayed recovery of the epibenthic community after a sustained period of hypoxia. In: Chandler, P.C., King, S.A., Boldt, J. (Eds.), *State of the Physical, Biological and Selected Fishery Resources of Pacific Canadian Marine Ecosystems in 2017*. Can Tech Rep Fish Aquat Sci 3266 (viii + 245 p).
- Craig, J.K., Crowder, L.B., 2005. Hypoxia-induced habitat shifts and energetic consequences in Atlantic croaker and brown shrimp on the Gulf of Mexico shelf. *Mar. Ecol. Prog. Ser.* 294, 79–94.
- Crawford, W.R., Pena, M.A., 2016. Decadal trends in oxygen concentration in subsurface

- waters of the Northeast Pacific Ocean. *Atmos-Ocean* 54, 171–192.
- Danovaro, R., Gambi, C., Dell'Anno, A., Corinaldesi, C., Fraschetti, S., Vanreusel, A., Vincx, M., Gooday, A.J., 2008. Exponential decline of deep-sea ecosystem functioning linked to benthic biodiversity loss. *Curr. Biol.* 18, 1–8.
- Darling, E.S., McClanahan, T.R., Cote, I.M., 2013. Life histories predict coral community disassembly under multiple stressors. *Glob Change Biol* 19, 1930–1940.
- Daskalov, G.M., Boicenco, L., Grishin, A.N., Lazar, L., Mihneva, V., Shlyakhov, V.A., Zengin, M., 2017. Architecture of collapse: regime shift and recovery in an hierarchically structured marine ecosystem. *Glob Change Biol* 23, 1486–1498.
- De'ath, G., 2002. Multivariate regression trees: a new technique for modeling species–environment relationships. *Ecology* 83, 1105–1117.
- Deutsch, C., Ferrel, A., Seibel, B., Pörtner, H.-O., Huey, R.B., 2015. Climate change tightens a metabolic constraint on marine habitats. *Science* 348, 1132–1135.
- Doney, S.C., Ruckelshaus, M., Duffy, J.E., Barry, J.P., Chan, F., English, C.A., Galindo, H.M., Grebmeier, J.M., Hollowed, A.B., Knowlton, N., Polovina, J., Rabalais, N.N., Sydeman, W.J., Talley, L.D., 2012. Climate change impacts on marine ecosystems. In: Carlson, C.A., Giovannoni, S.J. (Eds.), *Annu Rev Mar Sci. Annual Reviews*, Palo Alto, vol 4. pp. 11–37.
- Doya, C., Aguzzi, J., Chatzievangelou, D., Costa, C., Company, J.B., Tunnicliffe, V., 2016. The seasonal use of small-scale space by benthic species in a transiently hypoxic area. *J. Mar. Syst.* 154, 280–290.
- Drake, J.A., 1990. The mechanics of community assembly and succession. *J. Theor. Biol.* 147, 213–233.
- Drake, J.A., 1991. Community-assembly mechanics and the structure of an experimental species ensemble. *Am. Nat.* 137, 1–26.
- Emslie, M.J., Cheal, A.J., Johns, K.A., 2014. Retention of habitat complexity minimizes disassembly of reef fish communities following disturbance: a large-scale natural experiment. *PLoS One* 9, e105384.
- Frölicher, T.L., Laufkötter, C., 2018. Emerging risks from marine heat waves. *Nat. Commun.* 9, 650.
- Gasbarro, R., Chu, J.W.F., Tunnicliffe, V., 2017. Epibenthic community structure along a dissolved oxygen gradient. In: Chandler, P.C., King, S.A., Perry, R.I. (Eds.), *State of the Physical, Biological and Selected Fishery Resources of Pacific in 2016*. Can Tech Rep Fish Aquat Sci 3225.
- Giller, P.S., O'Donovan, G., 2002. Biodiversity and ecosystem function: do species matter? *Biol Environ* 102B, 129–139.
- Gotelli, N.J., 2000. Null model analysis of species co-occurrence patterns. *Ecology* 81, 2606–2621.
- Gotelli, N.J., Hart, E.M., Ellison, A.M., 2015. *Co-occurrence Analysis*. EcosimR Available at [www.ecosimr.org](http://www.ecosimr.org).
- Grundle, D.S., Timothy, D.A., Varela, D.E., 2009. Variations of phytoplankton productivity and biomass over an annual cycle in Saanich Inlet, a British Columbia fjord. *Cont. Shelf Res.* 29, 2257–2269.
- Harris, R.M.B., Beaumont, L.J., Vance, T.R., Tozer, C.R., Remenyi, T.A., Perkins-Kirkpatrick, S.E., Mitchell, P.J., Nicotra, A.B., McGregor, S., Andrew, N.R., Letnic, M., Kearney, M.R., Wernberg, T., Hutley, L.B., Chambers, L.E., Fletcher, M.-S., Keatley, M.R., Woodward, C.A., Williamson, G., Duke, N.C., Bowman, D.M.J.S., 2018. Biological responses to the press and pulse of climate trends and extreme events. *Nat. Clim. Chang.* 8, 579.
- Herlinveaux, R., 1962. Oceanography of Saanich Inlet in Vancouver Island, British-Columbia. *J. Fish. Res. Board Can.* 19, 1–37.
- Ito, T., Minobe, S., Long, M.C., Deutsch, C., 2017. Upper ocean O<sub>2</sub> trends: 1958–2015. *Geophys. Res. Lett.* 44 (9), 4214–4223.
- Jacox, M.G., Hazen, E.L., Zaba, K.D., Rudnick, D.L., Edwards, C.A., Moore, A.M., Bograd, S.J., 2016. Impacts of the 2015–2016 El Niño on the California Current System: early assessment and comparison to past events. *Geophys. Res. Lett.* 43, 7072–7080.
- Johnson, K.H., Vogt, K.A., Clark, H.J., Schmitz, O.J., Vogt, D.J., 1996. Biodiversity and the productivity and stability of ecosystems. *Trends Ecol. Evol.* 11, 372–377.
- Jørgensen, B.B., 1980. Seasonal oxygen depletion in the bottom waters of a Danish fjord and its effect on the benthic community. *Oikos* 34, 68–76.
- Keeling, R.F., Körtzinger, A., Gruber, N., 2010. Ocean deoxygenation in a warming world. *Annu. Rev. Mar. Sci.* 2, 199–229.
- Kodama, K., Oyama, M., Kume, G., Serizawa, S., Shiraiishi, H., Shibata, Y., Shimizu, M., Horiguchi, T., 2010. Impaired megabenthic community structure caused by summer hypoxia in a eutrophic coastal bay. *Ecotoxicology* 19, 479–492.
- Leitao, R.P., Zuanon, J., Villeger, S., Williams, S.E., Baraloto, C., Fortunel, C., Mendonça, F.P., Moullot, D., 2016. Rare species contribute disproportionately to the functional structure of species assemblages. *Proc R Soc B-Biol Sci* 283, 20160084.
- Levin, L.A., 2018. Manifestation, drivers, and emergence of open ocean deoxygenation. *Annu. Rev. Mar. Sci.* 10, 229–260.
- Manning, C.C., Hamme, R.C., Bourbonnais, A., 2010. Impact of deep-water renewal events on fixed nitrogen loss from seasonally-anoxic Saanich Inlet. *Mar. Chem.* 122, 1–10.
- Matabos, M., Tunnicliffe, V., Juniper, S.K., Dean, C., 2012. A year in hypoxia: epibenthic community responses to severe oxygen deficit at a subsea observatory in a coastal inlet. *PLoS One* 7, e45626.
- May, R.M., Levin, S.A., Sugihara, G., 2008. Complex systems: ecology for bankers. *Nature* 451, 893–895.
- McClain, C.R., Nunnally, C., Chapman, A.S.A., Barry, J.P., 2018. Energetic increases lead to niche packing in deep-sea wood falls. *Biol. Lett.* 14, 20180294.
- McCormick, L.R., Levin, L.A., 2017. Physiological and ecological implications of ocean deoxygenation for vision in marine organisms. *Phil. Trans. R. Soc. A* 375, 20160322.
- Mittelbach, G.G., Steiner, C.F., Scheiner, S.M., Gross, K.L., Reynolds, H.L., Waide, R.B., Willig, M.R., Dodson, S.I., Gough, L., 2001. What is the observed relationship between species richness and productivity? *Ecology* 82, 2381–2396.
- Moffitt, S.E., Hill, T.M., Roopnarine, P.D., Kennett, J.P., 2015. Response of seafloor ecosystems to abrupt global climate change. *PNAS* 112, 4684–4689.
- Nilsson, H.C., Rosenberg, R., 2000. Succession in marine benthic habitats and fauna in response to oxygen deficiency: analysed by sediment profile-imaging and by grab samples. *Mar. Ecol. Prog. Ser.* 197, 139–149.
- Nybakken, J., McDonald, G., 1981. Feeding mechanisms of west American nudibranchs feeding on Bryozoa, Cnidaria and Ascidiacea, with special respect to the radula. *Malacologia* 20, 439–449.
- O'Neill, B.J., 2016. Community disassembly in ephemeral ecosystems. *Ecology* 97, 3285–3292.
- Olesen, J.M., Bascompte, J., Elberling, H., Jordano, P., 2008. Temporal dynamics in a pollination network. *Ecology* 89, 1573–1582.
- Post, W.M., Pimm, S.L., 1983. Community assembly and food web stability. *Math. Biosci.* 64, 169–192.
- Pörtner, H.-O., 2010. Oxygen- and capacity-limitation of thermal tolerance: a matrix for integrating climate-related stressor effects in marine ecosystems. *J. Exp. Biol.* 213, 881–893.
- Purvis, A., Agapow, P.-M., Gittleman, J.L., Mace, G.M., 2000. Nonrandom extinction and the loss of evolutionary history. *Science* 288, 328–330.
- R Development Core Team, 2017. *R: A Language and Environment for Statistical Computing*. R Foundation for Statistical Computing, Vienna. [www.R-project.org/](http://www.R-project.org/).
- Rabalais, N.N., Diaz, R.J., Levin, L.A., Turner, R.E., Gilbert, D., Zhang, J., 2010. Dynamics and distribution of natural and human-caused hypoxia. *Biogeosciences* 7, 585–619.
- Ross, S.T., 1986. Resource partitioning in fish assemblages: a review of field studies. *Copeia* 1986, 352–388.
- Ross, T., 2017. La Niña, the blob and another warmest year. In: Chandler, P.C., King, S.A., Perry, R.I. (Eds.), *State of the Physical, Biological and Selected Fishery Resources of Pacific Canadian Marine Ecosystems in 2016*. Can Tech Rep Fish Aquat Sci.
- Ryan, J.A., Ulrich, J.M., 2017. *xts: eXtensible Time Series*. R package version 0.10-0. <https://CRAN.R-project.org/package=xts>.
- Saavedra, S., Reed-Tsochas, F., Uzzi, B., 2008. Asymmetric disassembly and robustness in declining networks. *Proc. Natl. Acad. Sci. U. S. A.* 105, 16466–16471.
- Sato, K.N., Levin, L.A., Schiff, K., 2017. Habitat compression and expansion of sea urchins in response to changing climate conditions on the California continental shelf and slope (1994–2013). *Deep-Sea Res Pt II* 137, 377–389.
- Sato, K.N., Andersson, A.J., Day, J.M.D., Taylor, J.R.A., Frank, M.B., Jung, J.-Y., McKittrick, J., Levin, L.A., 2018. Response of sea urchin fitness traits to environmental gradients across the Southern California oxygen minimum zone. *Front. Mar. Sci.* 5, 258.
- Scheffer, M., Bascompte, J., Brock, W.A., Brovkin, V., Carpenter, S.R., Dakos, V., Held, H., van Nes, E.H., Rietkerk, M., Sugihara, G., 2009. Early-warning signals for critical transitions. *Nature* 461, 53–59.
- Schluter, D., 1984. A variance test for detecting species associations, with some example applications. *Ecology* 65, 998–1005.
- Seibel, B.A., 2011. Critical oxygen levels and metabolic suppression in oceanic oxygen minimum zones. *J. Exp. Biol.* 214, 326–336.
- Sperling, E.A., Frieder, C.A., Levin, L.A., 2016. Biodiversity response to natural gradients of multiple stressors on continental margins. *Proc. R. Soc. B* 283, 20160637.
- Springer, A.M., Estes, J.A., van Vliet, G.B., Williams, T.M., Doak, D.F., Danner, E.M., Forney, K.A., Pfister, B., 2003. Sequential megafaunal collapse in the North Pacific Ocean: an ongoing legacy of industrial whaling? *PNAS* 100, 12223–12228.
- Stone, L., Roberts, A., 1990. The checkerboard score and species distributions. *Oecologia* 85, 74–79.
- Stramma, L., Schmidtke, S., Levin, L.A., Johnson, G.C., 2010. Ocean oxygen minima expansions and their biological impacts. *Deep-Sea Res Pt I* 57, 587–595.
- Stramma, L., Prince, E.D., Schmidtke, S., Luo, J., Hoolihan, J.P., Visbeck, M., Wallace, D.W.R., Brandt, P., Körtzinger, A., 2012. Expansion of oxygen minimum zones may reduce available habitat for tropical pelagic fishes. *Nature Clim Change* 2, 33–37.
- Sturdivant, S.K., Diaz, R.J., Cutter, G.R., 2012. Bioturbation in a declining oxygen environment, in situ observations from Wormcam. *PLoS One* 7, e34539.
- Thébault, E., Fontaine, C., 2010. Stability of ecological communities and the architecture of mutualistic and trophic networks. *Science* 329, 853–856.
- Torres-Beltrán, M., Hawley, A.K., Capelle, D., Zaikova, E., Walsh, D.A., Mueller, A., Scofield, M., Payne, C., Pakhomova, L., Kheirandish, S., Finke, J., Bhatia, M., Shevchuk, O., Gies, E.A., Fairley, D., Michiels, C., Suttle, C.A., Whitney, F., Crowe, S.A., Tortell, P.D., Hallam, S.J., 2017. A compendium of geochemical information from the Saanich inlet water column. *Sci Data* 4, 170159.
- Torres-Beltrán, M., Schein, T., Pachiadaki, M.G., Hallam, S.J., Edgcomb, V., 2018. Protistan parasites along oxygen gradients in a seasonally anoxic fjord: a network approach to assessing potential host-parasite interactions. *Deep-Sea Res Pt II* 156, 97–110.
- Tunnicliffe, V., 1981. High species diversity and abundance of the epibenthic community in an oxygen-deficient basin. *Nature* 294, 354–356.
- Ulrich, W., 2008. *Pairs – A FORTRAN Program for Studying Pair-wise Species Associations in Ecological Matrices*. [www.uni.torun.pl/~ulrichw](http://www.uni.torun.pl/~ulrichw).
- Vaquer-Sunyer, R., Duarte, C.M., 2008. Thresholds of hypoxia for marine biodiversity. *Proc. Natl. Acad. Sci. U. S. A.* 105, 15452–15457.
- Walsh, D.A., Zaikova, E., Howes, C.G., Song, Y.C., Wright, J.J., Tringe, S.G., Tortell, P.D., Hallam, S.J., 2009. Metagenome of a versatile chemolithoautotroph from expanding oceanic dead zones. *Science* 326, 578–582.
- Whitney, F.A., Freeland, H.J., Robert, M., 2007. Persistently declining oxygen levels in the interior waters of the eastern subarctic Pacific. *Prog in Oceanogr* 75, 179–199.
- Whyte, J.N.C., Carswell, B.I., 1982. Determinants for live holding the spot prawn *Pandalus platyceros*, Brandt. *Can. Tech. Rep. Fish. Aquat. Sci.* 1129, 29.
- Wishner, K.F., Seibel, B.A., Roman, C., Deutsch, C., Outram, D., Shaw, C.T., Birk, M.A., Mislán, K.A.S., Adams, T.J., Moore, D., Riley, S., 2018. Ocean deoxygenation and zooplankton: very small oxygen differences matter. *Sci. Adv.* 4, eaau5180.

- Worm, B., Barbier, E.B., Beaumont, N., Duffy, J.E., Folke, C., Halpern, B.S., Jackson, J.B.C., Lotze, H.K., Micheli, F., Palumbi, S.R., Sala, E., Selkoe, K.A., Stachowicz, J.J., Watson, R., 2006. Impacts of biodiversity loss on ocean ecosystem services. *Science* 314, 787–790.
- Yahel, G., Yahel, R., Katz, T., Lazar, B., Herut, B., Tunnicliffe, V., 2008. Fish activity: a major mechanism for sediment resuspension and organic matter remineralization in coastal marine sediments. *Mar. Ecol. Prog. Ser.* 372, 195–209.
- Zaikova, E., Walsh, D.A., Stilwell, C.P., Mohn, W.W., Tortell, P.D., Hallam, S.J., 2010. Microbial community dynamics in a seasonally anoxic fjord: Saanich inlet, British Columbia. *Environ. Microbiol.* 12, 172–191.
- Zavaleta, E., Pasari, J., Moore, J., Hernandez, D., Suttle, K.B., Wilmers, C.C., 2009. Ecosystem responses to community disassembly. In: Ostfeld, R.S., Schlesinger, W.H. (Eds.), *Year in Ecology and Conservation Biology 2009*. Blackwell Publishing, Oxford, pp. 311–333.
- Zeileis, A., Grothendieck, G., 2017. Zoo: S3 infrastructure for regular and irregular time series. *J. Stat. Softw.* 14 (6), 1–27. <https://doi.org/10.18637/jss.v014.i0>.